

HSPiP software as a powerful tool for optimization studies in chemical nanoengineering

Łukasz Lamch^{1*} , Krzysztof Gawarecki² , Dawid Szarpak¹, Kazimiera A. Wilk^{1*} 

¹ Wrocław University of Science and Technology, Faculty of Chemistry, Department of Engineering and Technology of Chemical Processes, Wybrzeże Wyspiańskiego 27, 50-370 Wrocław, Poland

² Wrocław University of Science and Technology, Faculty of Fundamental Problems of Technology, Institute of Theoretical Physics, Wybrzeże Wyspiańskiego 27, 50-370 Wrocław, Poland

*** Corresponding authors, e-mail:**

kazimiera.wilk@pwr.edu.pl

lukasz.lamch@pwr.edu.pl

Chemical Engineering Horizons and Perspectives. Article series endorsed by the Scientific Committee on Chemical and Process Engineering of the Polish Academy of Sciences, term 2024–2027.

Article info:

Received: 26 March 2025

Revised: 28 May 2025

Accepted: 05 June 2025

Abstract

The prediction of physicochemical parameters of novel compounds and their blends is an emerging problem in chemical nanoengineering, especially in the fields of fine chemicals and specialty polymers. Hansen solubility parameters in practice (HSPiP) software enables one to get valuable data from the known chemical structure on the basis of appropriate, standardized experiment, e.g. dissolution or swelling in a particular set of solvents. Herein we present a brief description of the recent applications of HSPiP software, supported by experimental and theoretical methods, including machine learning clusterization, aimed to solve technological and engineering issues. The present contribution aims to show the combined way of solvent clusterization for HSPiP studies for the determination of solubility parameters for novel surfactants, polymer blending toward drug nanocarriers as well as design of silicone-based polymer nanomatrix. The examples comprise the recent contribution of the groups' research, previously published or studied in current projects of our groups.

Keywords

Hansen solubility parameter, clustering, solvent selection, rationale nanoparticles, surface functionalization

1. INTRODUCTION

There is a great demand for prediction and description of solubility in chemical nanoengineering, especially in the fields of solvent selection for particular applications, design of polymer blends as well as surface science, including novel amphiphatic compound use toward solubilization and interfacial adsorption. In the field of process engineering, the question if the designed system really constitutes the optimal one is crucial. Therefore, any experimental findings must be supported with appropriate theoretical explanations. The previously indicated issues comprise the emerging ones, since there is a great demand for novel, more environmentally friendly, solvents (Milescu et al., 2020; Yu et al., 2021) and macromolecular nanomaterials, including nanocomposites, (Qin et al., 2019) as well as new reaction media (Kobayashi et al., 2020; Wieneke et al., 2012; Zhu et al. 2019) and surface modifiers (Barry et al., 2017). Different theories may not be comparable with each other, therefore there is a great demand for a systematic model, combining the possibly largest number of compounds, parameters and applications. One of the most general systems, based on the concept of solubility parameter by Hansen and group increment approaches, is HSPiP (Hansen solubility parameter in practice) software developed by Dr. Abbott, Dr. Hansen

and Dr. Yamamoto in 2009 (Abbott et al., 2020). Nowadays, it enables to predict not only the solubility parameter (δ) and its components, but also a large number of properties, including phase transition temperatures/enthalpies, dependence on mass solubilities, on temperature, flash point, partition coefficient and viscosity. The great potential of HSPiP is based on group increment methods enabling to estimate them for any structure given in SMILES notation. On the other hand, the significant drawback of HSPiP driven calculations is lack of possibility to estimate ionic interactions. Therefore, the basic software is practically useless for numerous compounds, e.g. organic salts like some surfactants or ionic liquids, metal complexes or amphoteric organics/inner salts (Kobayashi et al., 2020; Wieneke et al., 2012; Zhang et al., 2024; Zhu et al. 2019). Such drawbacks may be overcome by an appropriate combination of the software and other supporting methodologies, like conductometry in the case of organic-borne electrolytes (Kobayashi et al., 2020).

The use of predictive and simulative approaches is particularly attractive in the field of fine and specialty chemicals, due to a large amount of, mostly novel or even only theoretically described, various chemicals to be handled, high cost of the synthesis, demanding as low as possible experimental effort as well as the need for safer alternatives, especially for health



and agriculture applications (Ash and Ash, 2009; Ciriminna et al., 2024; Ledakowicz et al., 2024; Pollak, 2011; Szczęśna et al., 2022; Warszyński et al., 2022; Zhou and Metivier, 2023). High potential of HSPiP based methodologies is supported by computability with modern approaches as Quality by Design (QbD) and Quantitative Structure Activity Relationship (QSAR), enabling to identify critical parameters with the most significant impact on the desired output over product's lifecycle (Hussain et al., 2023b; Patil et al., 2024). Such possibilities, most commonly applied in pharmaceutical industry, may constitute a part of Process Analytical Technology (PAT) approaches, enabling the design of whole processes in chemical engineering with the crucial significance on product quality (Gerzona et al., 2022).

Herein, we explain the usefulness of HSPiP software, combined with different experimental (e.g. contact angle measurements, solubility, conductivity and thermal behavior) and theoretical (e.g. molecular modeling, machine learning clustering algorithms) methods, in solving various emerging technological and engineering problems. Our review is supported by the recent contribution of the groups' research on Hansen solubility parameter determination for new multicharge surfactants as crucial building blocks for nanoparticles fabrication, polymer blends for drug delivery nanosystems as well as silicone-based host nanomaterials for phthalocyanine-type derivatives, supported by machine learning approaches toward solvent selection.

2. THE BACKGROUND OF HSPiP

2.1. Hansen solubility sphere

In order to improve the original concept of cohesive forces and Hildebrand solubility parameter (δ), known also as total solubility parameter, the separate numbers, distinguishing dispersion (δ_D), polar (δ_P) and hydrogen bonding (δ_H) forces have been introduced (Abbott et al., 2020; Hansen, 2000; van Krevelen, 2009). It should be emphasized that each increment represents particular, well-known interactions: δ_D – represents, in general, van der Waals interactions, the dominating force in most interactions; δ_P – electrical attractions arising from dipole moments, existing in the major fraction of well-known organic chemicals (except for some hydrocarbons and perfluorated compounds) as well as δ_H – a specific type of polar interactions, distinguished due to scientific importance for electron exchange processes. Since the fourth type of interactions – ionic forces – constitute, mostly, the domain of aqueous environments and some crystals, the introduction of the fourth parameter does not seem to be useful. Moreover, the division of energy types in aqueous systems is still undergoing further research, leading to its better understanding. Therefore, Hansen solubility theory is practical for systems that do not involve significant amounts of water and there is a need to treat this solvent cautiously. The total solubility parameter for

a particular substance is composed of dispersion, polar and hydrogen bonding increments given by the simple equation:

$$\delta = \sqrt{\delta_D^2 + \delta_P^2 + \delta_H^2} \quad (1)$$

The distance ($\Delta\delta$) between two substances (subscripts 1 and 2) should be given by the geometrical distance between two points if the influence of each parameter (δ_D , δ_P and δ_H) was equal:

$$\Delta\delta = \sqrt{(\delta_{D2} - \delta_{D1})^2 + (\delta_{P2} - \delta_{P1})^2 + (\delta_{H2} - \delta_{H1})^2} \quad (2)$$

In fact, the influence of each component should be appropriately weighted, so the actual formula is:

$$(\Delta\delta)^2 = 4(\delta_{D2} - \delta_{D1})^2 + (\delta_{P2} - \delta_{P1})^2 + (\delta_{H2} - \delta_{H1})^2 \quad (3)$$

This is due to the experimentally proven fact that heat of mixing for dispersion forces is four times higher when compared with that of polar and hydrogen bonding. For any mixture, Hansen solubility parameters of δ_D , δ_P and δ_H comprise the average, weighted for % contribution, of the individual components. Typically, any substance may be represented by a point in three dimensional space, where each parameter is represented by an appropriate axis. There exists an additional, fourth, parameter – the radius (R) of the solubility sphere, representing the maximum distance from the center (point for “ideal” solubility of a particular substance) assuming its solubility. The most common method for determination of δ_D , δ_P and δ_H values as well as the radius of the sphere for any substance is mathematical analysis of its solubility in a set of different solvents by HSPiP software. Typically, a “good” solvent is rated 1, while a “bad” one – 0. The statistical selection of solvents as well as criteria for distinguishing “good” and “bad” environments to dissolve the given substance are the most challenging aspects of this method, although they may be “iterational”: it is possible to arbitrary select some solvents and add new ones (or their mixtures) to make fitting better. Typically, for a three dimensional system, a green dot represents the determined δ_D , δ_P and δ_H values for the studied substance (simply they may be denoted as [δ_D , δ_P , δ_H] like coordinates for 3D plot), blue dots – δ_D , δ_P and δ_H values for “good” solvents, i.e. situated inside the sphere, while red squares – such values for “bad” solvents, i.e. those outside the sphere. In order to quantitatively describe the analyzed solvents, the RED (Relative Energy Difference) number has been introduced by the equation:

$$RED = \frac{\Delta\delta}{R} \quad (4)$$

where $\Delta\delta$ denotes the distance, given by Equation (3), for a particular solute (i.e. the studied substance) – solvent system (regardless of whether the “solute” is really soluble or not), while R is the radius of the sphere for the studied substance. For a “good” solvent $RED < 1$, while for a “bad” one $RED > 1$; in general, RED value for the best solvent should be as low as possible, i.e. more close to 0.

In order to show all parameters in a convenient way as triangular graphs – Teas plots – values of δ_D , δ_P and δ_H should be converted:

$$\delta D = \frac{\delta_D}{\delta_D + \delta_P + \delta_H} \quad (5)$$

$$\delta P = \frac{\delta_P}{\delta_D + \delta_P + \delta_H} \quad (6)$$

$$\delta H = \frac{\delta_H}{\delta_D + \delta_P + \delta_H} \quad (7)$$

2.2. HSPiP for any molecule – Y–MB approach

Prediction of physicochemical properties of any molecule of a known structure, regardless of whether it really exists or not, poses a challenging task, even for well-known parameters like solubility parameter components of dispersion (δ_d), polar (δ_p), and hydrogen bonding (δ_h) forces, total solubility parameter (δ), melting point (MP), boiling point (BP), octanol-water partition coefficient (denoted as $\log(Kow)$) and aqueous solubility (denoted as $\log(S)$). Historically, there have been developed numerous approximations with the well-known Hoy's and Hoftyzer-van-Krevelen's methods (Abbott et al., 2020; Hansen, 2000; van Krevelen, 2009). Typically, such approaches are known as "group increment methods" since they utilize dividing a particular molecule or macromolecule into "building blocks" of the known contribution into the final value of a particular parameter. In an ideal situation, the total value, e.g. for components of dispersion forces into solubility parameter, comprise just a sum of particular values for structural "building blocks". On the other hand, an algebraic sum rarely provides reliable data, so appropriate corrections, e.g. utilizing the molar volume of the whole molecule, are needed. The weakest point of those methodologies is a very limited number of particular increment groups with known values of appropriate counterparts and a relatively large set of components, especially for polar chemicals motifs, with only roughly estimated numbers.

Nowadays, the most sophisticated method for estimation of numerous parameters for a very large group of organic molecules is Y–MB (Yamamoto Molecular Breaking). At first, it should be stated that this method is useful only for small molecules, i.e. with the current limit of 120 heavy atoms – atoms other than hydrogen, and its usage for polymers or large molecules may involve manual "splitting" of the given molecule into appropriate fragments with optimal ending motifs by the user. The greatest advantage of Y–MB method over the previous ones is that it allows software to automatically calculate appropriate values from the structure, provided by SMILES notation (Abbott et al., 2020). For other methods it is needed for the user to manually divide a molecule into groups of the known contributions, which may be challenging.

Solubility parameter components of dispersion (δ_d), polar (δ_p), and hydrogen bonding (δ_h) forces as well as total solubility parameter (δ) are combined with thermodynamic parameters

at 25 °C: enthalpy of vaporization (ΔH_{vap}), boiling point (T_b) critical temperature (T_{cr}) and molar volume (M_{vol}) by the following formulas:

$$\delta = \sqrt{\frac{\Delta H_{vap} - RT}{M_{vol}}} \quad (8)$$

$$\Delta H_{vap}(T=298K) = \Delta H_{vap}(T_b) \left(\frac{1 - 198.15}{T_{cr}} \right)^{0.38} \left(\frac{T_{cr}}{1 - \frac{T_b}{T_{cr}}} \right) \quad (9)$$

For not known molecules, T_{cr} values are estimated using the Y–MB group increment method. The value of δ_p is combined with the dipole moment (DM) and the molar volume (M_{vol}) by the Beerbower formula (note that the numerical parameter is revised for utilization by HSPiP software):

$$\delta_P = 36.1 \sqrt{\frac{DM}{M_{vol}}} \quad (10)$$

Preferably, δ_D values are strongly dependent on DM and T_{cr} (as previously stated – estimated using the Y–MB group increment method) and gathered in an appropriate database for the HSPiP calculations. On the other hand, δ_D may be calculated from refractive index (RI), when known:

$$\delta_D = \frac{RI - 0.784}{0.0395} \quad (11)$$

The most problematic is the determination of δ_H values since they cannot be simply combined with any known (and easily measurable) physicochemical parameter and, in fact, constitute a special type of polar interactions. On the other hand, we can use the estimated values of δ_d , δ_p and δ as well as Equation (1):

$$\delta_H = \sqrt{\delta^2 - \delta_D^2 - \delta_P^2} \quad (12)$$

The hydrogen bonding component is the most uncertain one since there is no sufficient theoretical background for its separate distinguishing, although its "existence" is proven and needed due to a large number of experimental data. In order to avoid inconveniences with over- or underestimated values, Y–MB method allows splitting δ_H into donor (δ_{HD})/acceptor (δ_{HA}) counterparts with a greater accuracy with experimental data:

$$\delta_H = \sqrt{\delta_{HD}^2 + \delta_{HA}^2} \quad (13)$$

For such extension, the formula for $\Delta\delta$ between two substances (subscripts 1 and 2) follows Equation (14).

$$(\Delta\delta)^2 = 4(\delta_{D2} - \delta_{D1})^2 + (\delta_{P2} - \delta_{P1})^2 + 2(\delta_{HD2} - \delta_{HD1})(\delta_{HA2} - \delta_{HA1}) \quad (14)$$

The latter extensions, Equations (13) and (14), are particularly useful for miscibility of two large molecular weight components, e.g. formation of polymer blends.

3. HSPiP IN SOLVENT SELECTION

3.1. Brief overview of current applications

Selecting a proper solvent is one of the most challenging approaches for current synthetic chemistry as well as chemical engineering and technology since most of the chemical or biochemical processes on the Earth occur in aqueous environment (Jiang et al., 2014). The noticeable advantage for the predictive modeling software applications is the “trial-and-error” approach avoidance that are time-consuming and only provide the most suitable solvent from within the limited experimental data set (Petchey et al., 2018). The most sophisticated methods, utilizing Hansen solubility parameters in Practice (HSPiP) software, may be utilized for optimization studies of solvent-borne reaction mixtures (Jiang et al., 2014; Petchey et al., 2018; Tripathi et al., 2018; Yin et al., 2021), extraction/solubilization of particular compounds, comprising one type of chemical molecules (Laboukhi-Khorsi et al., 2017; Shakeel et al., 2021a; 2021b) as well as complicated mixtures (Díaz de los Ríos et al., 2022; Novo and Curvelo, 2019; Soyemi and Szilvási, 2023). In relation to water, organic solvents reveal a wide spectrum of properties responsible for various structures, polarities, as well as interfacial energy magnitudes. The theoretical values of a given solvent/solute compatibility can be determined from the total cohesive energy density, measured in evaporation experiments by the cohesion breaking up between the molecules (Bapat et al., 2021; Qin et al., 2019; Wieneke et al., 2012). Hansen solubility parameters constitute a profound concept to diminish the use of toxic solvents in a variety of industrial and research applications, including membrane processing, pharmaceuticals, cosmetics, and obtaining the solubility properties of biomass-derived solvents compared to toxic petro-based derivatives (Barry et al., 2017; Milescu et al., 2020; Yu et al., 2021).

3.2. HSPiP for greener solvent systems

Numerous organic solvents, including very valuable highly polar ones, can be potentially hazardous, even despite their low volatility. One example is dimethyl formamide (DMF), widely used as solvent for fiber-dyeing and printing applications since it can dissolve several polymers, including polycarbonates, some polyamides and polyurethanes, known for numerous hazards to human health (acute toxicity, irritancy to skin, reprotoxicity and potential carcinogenicity – class 2A). Therefore, there is an emerging need to replace it with safer and more environmentally friendly alternatives. Typical trial-and-error experiments are useless in these fields, due to limited effectiveness, especially for solvent mixtures, and growing number of accessible solvents. Therefore, determination in particular polymers of solubility parameter components (δ_d , δ_p and δ_h) as well as radius of solubility sphere (R) utilizing simple solubility experiment with a limited number of solvents and HSPiP offers a smart alternative. Such an approach (Yu

et al., 2021) enabled to find safer alternatives for DMF as polyurethane solvent, including specific mixtures of cyclohexanone with *n*-buthyl acetane (85:15, v:v) and cyclopentanone or cyclohexanone with dimethylsulfoxide (54:46, v:v). Solvents, including aromatic, petrochemically-derived ones, are also used as reaction media, e.g. in amidation processes. Utilizing a similar approach and HSPiP software, *p*-cymene has been found as the general alternative for toluene in catalyzed reaction between various carboxylic acids and amines (Milescu et al., 2020). The growing market of contact adhesives is also connected with extended research on finding appropriate alternatives for typical solvents hazardous to health, like toluene, xylene and methylene chloride. An extended HSPiP-based studies enabled to find triple solvent mixtures for dissolving particular resins and rubbers, aiming to reduce volatile organic solvent emissions from contact resin applications (Barry et al., 2017). It should be emphasized that the aforementioned studies show the great potential of HSPiP-based approaches toward solvent selection in the applied disperse systems, chemical nanoengineering, specialty polymer and coating technologies as well as in chemical technology (reaction media), especially due to minimized experimental effort and direct response which solvent/solvent mixture constitute the optimal one.

3.3. Optimization studies for crystallization of new multicharge surfactants, crucial building blocks for nanoparticle engineering

Due to their amphiphilic character, surfactants are particularly difficult to be purified, although careful removal of any impurities, organic and inorganic ones, is crucial for their surface activity measurements at interfaces (Lamch et al., 2023, 2025). Typically, surfactants, as solids, are purified by repeated crystallization from various solvents or solvent mixtures; the use of column chromatography is limited by their high affinity to any surfaces. Sometimes it is possible to heat surfactant in an appropriate solvent, typically up to its boiling point under reflux, until complete dissolution and keep at room or reduced (e.g. in freezer) temperature to induce crystallization. On the other hand, sometimes dual solvent approach is needed: typically surfactant is dissolved in a minimum amount of “good” solvents (i.e. solvent which completely dissolves surfactant), followed by gradual adding of “poor” solvent (i.e. solvent that does not dissolve surfactant) until slight turbidity appears. The introduction of “poor” solvent into “good” one may be performed at room or elevated (e.g. boiling point under reflux) temperature, while crystallization typically occurs at room or reduced temperature. For some surfactants it may be beneficial to utilize an opposite approach: an introduction of a “good” solvent into a slurry of the compound in a “poor” solvent, until the mixture becomes completely transparent (Lamch et al., 2023, 2025).

For our example we chose three multicharged cationic surfactants of a dicephalic type, i.e. possessing one hy-

drophobic tail and two hydrophilic headgroups, comprising exclusively carbon atoms with an exception for hydrophilic quaternary amine headgroups and counterions: 2-alkyl-N,N,N',N',N'-hexamethylpropan-1,3-ammonium dibromides (C_n -D C NMe₃Br). For the characterization of this unique class of surfactants, with potential applications e.g. as gene or drug delivery nanosystems, it was necessary to devise appropriate purification steps in order to get compounds of sufficiently high purity. In order to systematically study solubility of surfactants with different alkyl chain lengths ($n = 10, 12$ or 14), Hansen solubility parameters of the mentioned compounds were determined using the sphere method (Szarpak et al., 2024). The modular synthetic route for C_n -D C NMe₃Br surfactants, described in (Lamch et al., 2025), involves alkylation of dimethyl malonate, followed by reduction of the obtained intermediate and hydroxyl motifs exchange into bromide ones as well as final quaternization with trimethylamine. It is worth noticing, that for the multistep synthetic route

appropriate rational crystallization processes are essential in order to remove any traces of impurities significantly impacting surfactants' performance at interfaces.

Solubility of surfactants was probed utilizing simple solubility test (20 mg of surfactant per 2 ml of solvent; 1 min of sonication, followed by keeping samples at room temperature for 48 h) in 30 different solvents with assigning values 1 for soluble and 0 for insoluble. The obtained results were plotted in three dimensional space as well as Teas plots (see Table 1 and Fig. 1) in order to determine solubility parameter components (δ_D , δ_P and δ_H) as well as radius of solubility sphere (R) for the studied surfactants. It is worth noticing that only for four solvents (1-propanol, 1-butanol, N-methyl diethanolamine and propylene glycol monomethyl ether) there were differences in surfactant solubilities dependent on alkyl chain lengths.

Taking into account the determined values of Hansen solubility parameters (see Table 2) the studied surfactants are

Table 1. The set of solvents used for solubility probing with scores for particular surfactants C_n -D C NMe₃Br (for the structure see Table 2).

Solvent	δ_D , MPa ^{0.5}	δ_P , MPa ^{0.5}	δ_H , MPa ^{0.5}	Score		
				$n = 10$	$n = 12$	$n = 14$
Methanol	14.7	12.3	22.3	1	1	1
Diethyl ether	14.5	2.9	4.6	0	0	0
Acetonitrile	15.3	18	6.1	0	0	0
Methylene dichloride	17	7.3	7.1	0	0	0
Formamide	17.2	26.2	19	1	1	1
Ethyl acetate	15.8	5.3	7.2	0	0	0
Toluene	18	1.4	2	0	0	0
2-Propanol	15.8	6.1	16.4	0	0	0
2-Butanol	15.8	5.7	14.5	0	0	0
Chloroform	17.8	3.1	5.7	0	0	0
Dimethyl sulfoxide	18.4	16.4	10.2	1	1	1
Tetrahydrofuran	16.8	5.7	8	0	0	0
Ethylene Glycol	17	11	26	1	1	1
1-Butanol	16	5.7	15.8	0	0	1
Acetone	15.5	10.4	7	0	0	0
Ethanol	15.8	8.8	19.4	1	1	1
Cyclohexane	16.8	0	0.2	0	0	0
p-Xylene	17.6	1	3.1	0	0	0
Heptane	15.3	0	0	0	0	0
Dimethyl formamide	17.4	13.7	11.3	1	1	1
1-Propanol	16	6.8	17.4	1	0	1
3-Methoxy-3methyl butanol	16	6.3	12.9	0	0	0
Propylene carbonate	20	18	4.1	1	1	1
Propylene glycol monomethyl Ether	15.6	6.3	11.6	0	0	1
Methyl diethanolamine	16.8	8.3	17.6	1	0	1
1-Pentanol	15.9	5.9	13.9	0	0	0
Ethylene glycol monoethyl ether	15.9	7.2	14	1	1	1
Methylethanolamine	16.8	8.7	16.4	0	0	0
Dimethyl ethanoloamine	16.1	9.2	14	0	0	0
Water	15.5	16	42.3	1	1	1

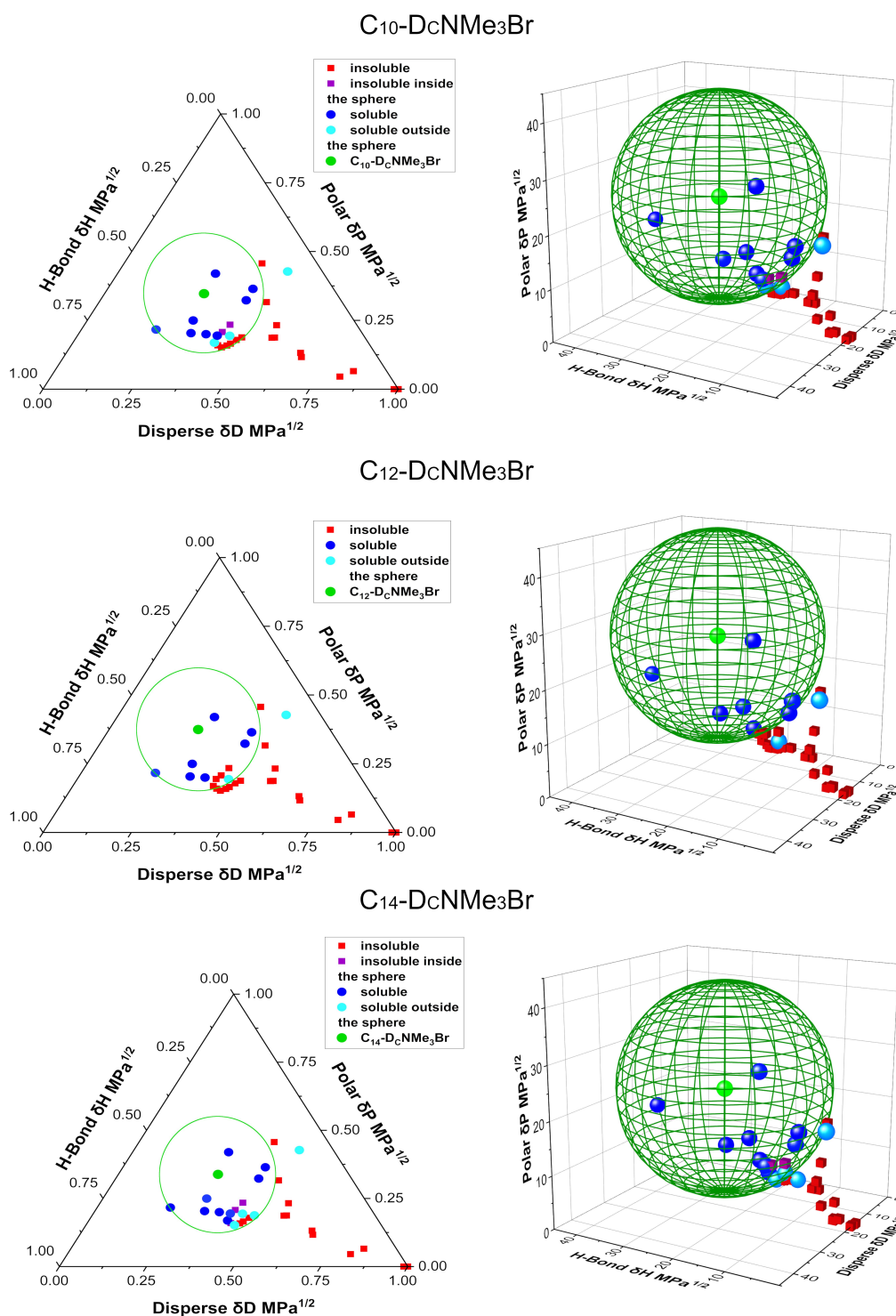
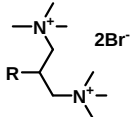


Figure 1. Three dimensional and Teas plots for the determination of Hansen solubility parameters of the studied dicephalic-type surfactants (for the structure see Table 2).

characterized by high tendency to interact by London ($\delta_D \approx 18-19.5 \text{ MPa}^{0.5}$), polar ($\delta_P \approx 22.5-26.5 \text{ MPa}^{0.5}$) and hydrogen bonding ($\delta_H \approx 25-26 \text{ MPa}^{0.5}$) forces. Such findings are in good agreement with amphiphatic structure of surfactants, comprising both hydrophobic (non-polar) and hydrophilic (polar) counterparts. The purification process should comprise pairs of solvents, exhibiting strong interactions by dominant

dispersion forces (relatively high value of $\delta_D \approx 14-16 \text{ MPa}^{0.5}$) as well as both polar and non-polar interactions (values of $\delta_D \approx 14-16 \text{ MPa}^{0.5}$ and δ_P or $\delta_H \approx 16-18 \text{ MPa}^{0.5}$). Repeated recrystallization from aforementioned mixtures of solvents enables one to remove both hydrophilic and hydrophobic impurities. Such findings provided the successful crystallization processes from 2-propanol ($\delta_D = 15.8 \text{ MPa}^{0.5}$,

Table 2. Structures, abbreviations and the determined HSPs values for the studied dicephalic-type surfactants.

Structure and name	R	Abbreviation	δ_D , MPa ^{0.5}	δ_P , MPa ^{0.5}	δ_H , MPa ^{0.5}	R_0
 2-alkyl-N,N,N,N',N',N'-hexamethyl- propan-1,3-ammonium dibromides	C ₁₀ H ₂₁	C ₁₀ -D _C NMe ₃ Br	19.2	23.8	25.6	19.9
	C ₁₂ H ₂₅	C ₁₂ -D _C NMe ₃ Br	17.7	26.3	26.2	19.9
	C ₁₄ H ₂₉	C ₁₄ -D _C NMe ₃ Br	19.1	22.6	25.1	19.9

$\delta_P = 6.1$ MPa^{0.5}, $\delta_H = 16.4$ MPa^{0.5}) – ethyl acetate ($\delta_D = 15.8$ MPa^{0.5}, $\delta_P = 5.3$ MPa^{0.5}, $\delta_H = 7.2$ MPa^{0.5}) and acetonitrile ($\delta_D = 15.3$ MPa^{0.5}, $\delta_P = 18$ MPa^{0.5}, $\delta_H = 6.1$ MPa^{0.5}) – to diethyl ether ($\delta_D = 14.5$ MPa^{0.5}, $\delta_P = 2.9$ MPa^{0.5}, $\delta_H = 4.6$ MPa^{0.5}) mixtures. It should be emphasized that all solvents chosen for crystallization are scored as “poor” according to solubility probing. A significant amount of surfactant (e.g. above 5% by weight) may be dissolved in the abovementioned mixtures only at elevated temperatures, allowing formation of crystals when left at room temperature.

3.4. Solubility parameters for ionic liquids

Ionic liquids comprise a very potent group of “green” alternatives for typical polar solvents, due to high boiling points and, thus, low vapor pressure, electroconductivity and high thermal stability. Their usefulness is particularly significant as novel electrolytes, reaction media and separation solvents. In the field of typical HSPs, they constitute a group of “difficult” solvents, since Y–MB approach does not take into account ionic interactions. Therefore, it is not possible to directly predict their properties, especially solubility sphere coordinates, on the basis of the knowledge of their chemical structure. On the other hand, there exist complementary methodologies, enabling to determine HSPs for ionic liquids: estimation of ionicity by Walden plots (Kobayashi et al., 2020) as well as inverse gas chromatography (Zhu et al., 2019). It should be noted that inverse gas chromatography has become one of the basic methodologies for determination of HSPs so nowadays some data, e.g. specific retention volumes, for the predicted compounds are available in HSPiP software (Abbott et al., 2020). Moreover, there exist numerous empirical or semi-empirical relationships, combining e.g. values of critical parameters for liquids (temperature and volume) with data from inverse gas chromatography, especially second virial coefficient (Chen et al., 2012; Wang et al., 2013; Zhu et al., 2019). The measurement involves the use of different “probes” of known parameters to determine the Flory-Huggins interaction parameter at various temperatures. Moreover, inverse gas chromatography allows to distinguish “good” and “poor” solvents for particular ionic liquids. The dependence of the

conductivity on the viscosity, known as Walden plots, enabling to study the ionic liquids dissociation rates, is more sophisticatedly connected with HSPs. For such considerations, “poor” and “good” solvents were given scores from 1 to 6, respectively. Moreover, “good” solvents were additionally put into three groups, dependent on Walden plot constants (Kobayashi et al., 2020). Combination of Walden plots with HSPiP software leads to determining the donor (δ_{HD})/acceptor (δ_{HA}) counterparts of hydrogen bonding for the appropriate ionic forms.

The considerations of HSPs for ionic liquids also showed an emerging need for appropriate solvent selection and dividing them into various subgroups. Further investigations may solve important technological issues, e.g. finding novel electrolytes for electrochemical devices as well as antistatic agents with the minimal experimental effort.

3.5. Machine learning approach to determine Hansen solubility parameters

The machine learning approach has gained much attention in various disciplines and led to a breakthrough in data science. These techniques can be divided into *supervised* and *unsupervised* learning. In the former, the algorithms work on datasets with assigned labels. The model minimizes the loss function, which measures the error between its predictions and the actual labels. In order to keep the model general (i.e. prevent *overfitting*), models are tested for “unseen” portion data, which is separated into the *validation set*. An important class of supervised learning methods is the *deep learning* approach with artificial neural networks (ANN). In this case, the data enter the input layer of the ANN and is processed by the hidden layers into the final, output layer (Chollet, 2021). This approach is very effective in solving specified tasks. In the unsupervised learning methods, the algorithms work on unlabeled data, trying to get the underlying structure (finding some patterns) (Patel, 2019). This approach is often used to divide datasets into distinct groups (clusters) containing similar instances (with respect to given features). Such a clustering procedure can be performed e.g. within the K-means, Hierarchical Clustering, DBScan (Patel, 2019), or Self-Organizing Map (SOM) (Kohonen, 1982, 2013) algorithms.

Machine-learning techniques can be utilized in chemistry on multiple levels and they are very promising to enhance studies on solvents. Such methods can be used to extract new information from existing empirical data, getting correlations that are difficult to find with standard statistical methods.

There are various studies aimed at predicting the values of the HSPs from the other properties that characterize a given solvent (Li et al., 2024; Mostafa et al., 2024; Wojeicchowski et al., 2022). This can be done based on e.g. the COSMO-RS (conductor-like screening model for realistic solvents) descriptors (Li et al. 2024; Wojeicchowski et al., 2022). In fact, the factorial regression approach showed promising results in predicting the HSPs from the σ moments and the COSMO-RS parameters (Wojeicchowski et al., 2022). Furthermore, finding the HSPs can be supported by combining COSMO-RS with the Group Contribution methods (Li et al., 2024). It has also been shown that the Deep Neural Network model and the Extreme Gradient Boosting Regressor approach are effective in predicting HSPs (Li et al., 2024).

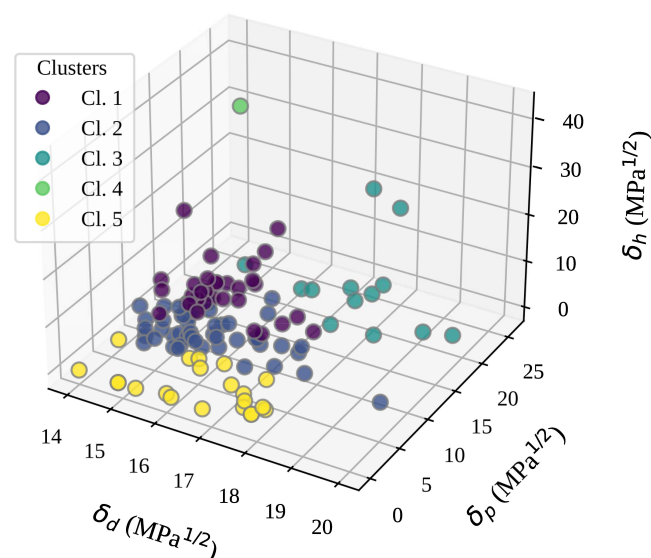
3.6. Solvent selection by machine learning algorithms

The machine learning techniques can also be harnessed for optimal solvent selection. For example, the clustering based on the SOM algorithm was used to implement the program which seeks for green alternatives for a given solvent (Sels et al., 2020). In another work (Lan et al., 2014), clusterization with the K-means algorithm was performed to correlate the solvent parameters with the gelation abilities of 1,3:2,4-dibenzylidene sorbitol.

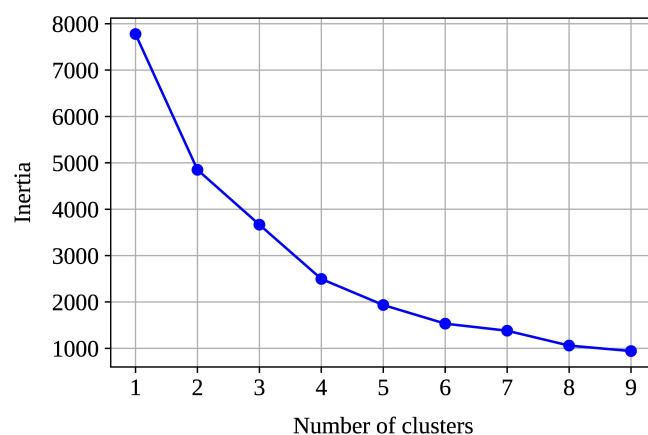
For substances of not known Hansen solubility sphere coordinates, it is beneficial to initially sample the Hansen space in a (possibly) uniform way. Therefore, a plausible choice involves solvents representing various groups (clusters). Here, we present an illustrative example, where we use K-means clustering algorithm to find groups of similarity in a set of 114 solvents. As shown in Fig. 1a, we represent the solvents as points defined by the HSP (δ_D , δ_P , δ_H) coordinates.

In this algorithm, the user needs to set the number of clusters, which we estimate using the so-called *elbow method*. To measure how well a given dataset is divided into clusters, one can use the *inertia* parameter, which is the sum of the within-cluster-variations of all clusters (Patel, 2019). The smaller inertia means better clustering. Its value decreases with an increasing number of clusters (see Fig. 2b). In the elbow method, the optimal number of clusters is assumed to be the point when the decrease begins to significantly slow down (hence the impact of further division gets smaller). As can be seen in Fig. 2b for the considered solvents, 5 is a reasonable choice for the number of clusters. We used this value in Fig. 2a, where the solvents are assigned to one of the 5 groups (and plotted with the corresponding colors). In calculating the distance between points for the clustering, we took the weight “2” for δ_D , which is consistent with Eq. (3).

Particular clusters correspond with different types of solvents. Cluster “1” comprises 32 solvents and represents compounds exhibiting values of δ_D and δ_H above ca 15 MPa^{0.5} and ca 12 MPa^{0.5}, respectively, with relatively lower values of δ_P (typically below 10 MPa^{0.5}). Chemically, those compounds constitute alcohols and their derivatives (e.g. esters or ethers) comprising at least one free hydroxyl motif – this structure explains high values of δ_H . Cluster “2” constitutes the largest



(a) HSPs of solvents – finding clusters



(b) Elbow method for optimal number of clusters

Figure 2. (a) Solvents represented via the Hansen solubility parameters, assigned to 5 clusters and (b) the K-Means inertia parameter as a function of the number of clusters.

group (47 solvents), characterized by values of δ_D above ca 15 MPa^{0.5} and relatively lower values of δ_P and δ_H . This group comprises various esters and ethers, including cyclic ones, as well as ketones, characterized by polar structure. Cluster "3" – 12 solvents – constitute a group of compounds with values of δ_D and δ_P above ca 15 MPa^{0.5}, such as acetonitrile, various cyclic esters, dimethylsulfoxide (DMSO) and *N,N*-dimethylformamide (DMF). This group may be roughly described as aprotic polar solvents. Water, due to the extreme value of δ_H (42.3 MPa^{0.5}), was denoted as the sole compound in cluster "4". And, finally, cluster "5" comprises compounds with values of δ_D above ca 15 MPa^{0.5} and relatively low (between 0 and 5 MPa^{0.5}) values of δ_P and δ_H . This group is dominated by hydrocarbon-based solvents, both aliphatic, cycloaliphatic and aromatic, as well as some ethers, esters and ketones, especially those with long or branched hydrocarbon chains.

Clusterization has a significant impact on the initial choice of solvents for experimental determination of HSPs by the sphere method. The optimal choice should involve solvents from all clusters, if possible. Such an approach assumes the adequate counting of all the aforementioned interactions and, therefore, provides the most accurate determination of the sphere coordinates [δ_D , δ_P , δ_H] as well as the radius (*R*). To recall, our previously mentioned determination of HSPs for dicephalic surfactants C_n -D_CNMe₃Br – see Section 3.3 – took into account the representatives from all 5 clusters. It is worth noticing that only some solvents (1-propanol, 1-butanol, *N*-methyl diethanolamine and propylene glycol monomethyl ether) from the cluster "1" (alcohols and their derivatives) exhibited any differences in solubility between particular surfactants of varying alkyl chain lengths. Such behavior may arise from differences in δ_D values between, particularly, C_{12} -D_CNMe₃Br (this compound is characterized by slightly, by ca 1.5 MPa^{0.5}, lower δ_D values when compared with other surfactants) and the mentioned solvents. Our findings confirmed the usefulness of clustering approaches in HSPs studies and optimization toward technological applications.

4. HSPiP CALCULATIONS FOR POLYMER BLENDS

In general, blending of polymers is a tricky task, since it is difficult to predict if particular macromolecular compounds are thermodynamically miscible ("blendable"). Even if they form a macroscopically uniform mixture, it could undergo slow separation processes, i.e. "frozen" structure turns into its thermodynamically stable state. HSPiP is successfully applied in regards to microheterogeneous mixtures, because it is gaining more attention in the sectors of contaminated water purification, as it provides better biocompatibility and scalability, making it possible to design more simple and cost-effective methodologies for pharmaceutical industry (Afzal et al., 2022; Hussain et al., 2023a, 2023d; Venkatesan et al., 2022). Our consider-

ations are supported with dissolving of the real technological problem, comprising the design of suitable polymer nanomatrix (Lamch, 2018) for delivery of three different biologically active compounds of natural (curcumin and resveratrol) or biotechnological (mitomycin C) origin (Lamch and Szklarz, 2024; Lamch and Szukiewicz, 2024; Weźgowiec et al., 2025).

4.1. Blending of polymers for their strong adhesion between them by HSPiP

Polymer blending, according to HSPiP theories, may be divided into two general cases: mixing in the bulk phase and at the surface, characteristic for adhesion. The first case resembles a polymer – solvent system with particular polymer chains tangled with each other. In contrast to low molecular weight solvents/host molecules, the calculation of standard Hansen solubility parameter distance (see Equation (3) in Section 2.1) may often be misleading. Often better results for polymer blends are obtained when hydrogen bonding component (δ_H) is divided into donor/acceptor interactions – see Equations (13) and (14) in Section 2.2. HSPiP software provides polymer miscibility calculator, taking into account molecular weights of mers (building blocks) and polymers as well as temperature in order to show when formation of thermodynamically stable polymer blend is possible (Abbott et al., 2020). HSPs for polymer blends may be probed by the standard sphere method, utilizing a set of solvents to dissolve or swell the existing mixture. This approach enabled to carefully study hydrogenated nitrile rubber/ ethylene propylene diene monomer rubber (HNBR/EPDM) blends with weight ratio of each component varying from 0 to 100% (Jiang et al., 2022). A similar approach, comprising studies of swelling behavior, was used to study thiol-ene networks toward HSPs and miscibility parameter determination (Bongiardina et al., 2021). The second case – surface blending of polymers – is the principle for strong adhesion between polymers. The real, strong adhesion between two polymers which is connected with energy of 100–1000 J/m² is dependent on polymer chains getting and staying entangled. Polymers should not only possess similar values of HSPs, but also be thermodynamically more stable in an extended state when compared with closed in upon themselves as well as (at least at the surface) treated with appropriate factor, triggering formation of entangled chains like solvent, heating or friction (Abbott et al., 2020).

4.2. Polymer plasticization toward drug nanocarriers

The growing interest of naturally-derived raw materials for polymers has significant impact not only on plastic industry, since polylactide constitutes one of the most common filaments for 3D printing, but also on pharmaceutical industry, due to unique properties of some polyesters as drug carrier nanomatrices. Polymer nanomatrix plasticization toward drug delivery nanosystems is multifactor optimization task, comprising: (i) the consideration of mutual compatibility between

the polymer and the plasticizer; (ii) the efficiency of the blended polymers to incorporate the drug molecules; (iii) the determination of plasticization process mode (solvent-based or hot plasticization) and (iv) the choice of appropriate solvent or solvent mixture. For nanoprecipitation-based preparation methodology the solvent must be volatile (boiling point at least 15–20 °C lower than that of water), when it is removed by evaporation, completely water miscible and providing broad ranges of payload and polymer solubility. All of the aforementioned considerations may be supported by HSPiP calculation, with the help of solvent clustering efforts. Such an approach is particularly important for scalable, industrial processes, very susceptible to suboptimal conditions/compositions, leading to e.g. accumulation of precipitated polymer films or chunks.

For our example we chose three different multifunctional drugs: curcumin (CUR), resveratrol (RES) and mitomycin C (MMC) of amphiphilic or hydrophobic character, encapsulated in core-shell nanoparticles with polyester matrix composed of poly(L-lactide) (PLLA), poly(lactide-co-glycolide) (PLGA) and/or poly(ethylene succinate) (PES) and stabilizing layer of newly devised hydrophobically functionalized polyelectrolytes (HF-PEs). The key point of the studied drugs is a high tendency to interact by dispersion (London) and hydrogen bonding forces, despite their different aqueous solubilities (good for MMC and poor, pH dependent for CUR and RES).

Our current contribution is focused on the optimization studies for scalable methodologies in batch-type equipment or membrane-assisted process – see our published papers (Lamch and Szklarz, 2024; Lamch and Szukiewicz, 2024; Weźgowiec et al., 2025) – comprising various aspects: mutual compatibility in drug – polymer nanomatrix – polymeric (oligomeric) plasticizer, the determination of optimal preparation temperatures and solvent/solvent mixtures choice, studied with HSPiP software. The calculation of $\Delta\delta$ (Y-MB method, HSPiP) for different polymer (PLLA, PLGA and PES) combinations – see Fig. 3 – showed that any of the aforementioned compounds may play the role of plasticizer to each other, due to very good compatibility ($\Delta\delta < 3 \text{ MPa}^{0.5}$). Since the use of PES as a single polymer nanomatrix building block is unfavorable, we calculated weight percent solubility of drugs in PLGA and PLLA in the temperature range of 25–100 °C. MMC, due to its susceptibility to degrade at elevated temperatures, was not studied in this way. Our results clearly show that CUR solubility in polymer (better in PLLA than in PLGA) matrix is highly temperature dependent, and it is very beneficial to prepare nanocarriers at elevated temperatures, followed by their rapid cooling to avoid recrystallization in nanocarrier cores. For RES such effect is far less significant so, taking into account possible degradation of PES oligomer (plasticizer), encapsulation is preferred to be performed at room temperature. For appropriate solvents, we performed multi-criteria analyses, taking into account boiling point, safety, miscibility with water and the Hansen solubility parameter distance from the polymer. To recall, an optimal solvent or solvent mixture should be characterized by as low as possible

(preferably $< 10 \text{ MPa}^{0.5}$) distance from the polymer, boiling point between ca 45–80 °C to enable easy evaporation from an aqueous system, complete miscibility with water and nontoxicity. Our studies indicate that the best solvent for any polymer (PLLA, PLGA) or oligomeric plasticizer (PES) is acetone, due to low Hansen solubility parameter distance ($< 5 \text{ MPa}^{0.5}$), miscibility with water, appropriate boiling point (56 °C) and nontoxicity. The second choice constitutes tetrahydrofuran, characterized by slightly higher, but acceptable, values of boiling point (66 °C) and the distance (between 5 and $10 \text{ MPa}^{0.5}$). Taking into account the relatively high boiling point (82 °C) and difficulties in removal from aqueous solution by evaporation, acetonitrile is a less favorable choice, although it is characterized by low Hansen solubility parameter distance (below or around $5 \text{ MPa}^{0.5}$).

Our studies clearly show excellent usefulness of HSPiP software toward optimization of scalable processes with high potential in the fine chemicals industry. It should be emphasized, that, especially when the used chemicals are unstable and/or expensive, the utilization of predictive software and approaches can significantly reduce the number of time-consuming and difficult experimental efforts. The designed methodologies of core-shell nanocarrier preparation, both membrane-assisted (Weźgowiec et al., 2025) and performed in batch-type vessel equipment (Lamch and Szklarz, 2024; Lamch and Szukiewicz, 2024), met all the known requirements in the fields of scalability, process parameter optimization as well as selection of plasticizer and solvent.

5. HANSEN SOLUBILITY PARAMETER AT INTERFACES

The interfacial phenomena may be described and explained by HSPiP software in various biomedical and bioengineering (Altamimi et al., 2022; Hussain et al., 2023b, 2023c, 2023d) fields. On the other hand, surface energy measurements (AlQasas et al., 2023) as well as viscosimetry or inverse gas chromatography techniques (Kobayashi et al., 2020; Malpani et al., 2011; Zhu et al., 2019) may be helpful for the determination of HSPs. It should be emphasized that the aforementioned applications of HSPs are getting more and more scientific and technological interest, especially in the fields of coating and adhesive industries, cosmetics and pharmacy.

5.1. The relationship between solubility and contact angle

Wetting of surfaces is a physical phenomenon with a great impact on numerous applications: hydrophobization/hydrophilization, coatings, adhesives, paints and many other. The crucial parameter for characterization of wetting performance is the contact angle, and its hysteresis, of particular liquid drop on the studied surface. The surface of the solid, e.g. glass, may also be characterized by HSP coordinates [δ_D , δ_P , δ_H] since surface energy, strictly

connected with contact angle, is often broken down into appropriate subcomponents. The simplest way to determine HSPs is to probe which liquids completely wet the surface (contact angle 0° , “good” solvents with score value “1”) and which do not (contact angle above 0° , “poor” solvents with score value “0”). For such considerations it is needed to state that only perfect wetting (contact angle 0°) may be scored “1” (Lazghab et al., 2005), although different approaches are also possible (Fujiwara et al., 2019; Tsutsumi et al., 2019). Another point are technical difficulties in determination of contact angles with values not exceeding a few degrees. The data for sufficient number of different solvents (see Section 3 for detailed information about solvent choice for

solubility probing) enables HSPiP software to determine Hansen solubility parameters for surface similarly to solids dissolved in solvents (Abbott et al., 2020). In fact, the distinguishing between a “good” and a “poor” solvent is a more complicated task. Very good wetting corresponds to a zero equilibrium contact angle, as the liquid will get spread spontaneously and wet the substrate completely (Lazghab et al., 2005). Many reports (Fujiwara et al., 2019; Tsutsumi et al., 2019) used the contact angle threshold to differentiate between a good and a bad solvent in order to estimate the Hansen solubility parameter. Tsutsumi et al. (2019) evaluated the contact angle by means of the Washburn equation, and a threshold for dividing the poor solvents from the good

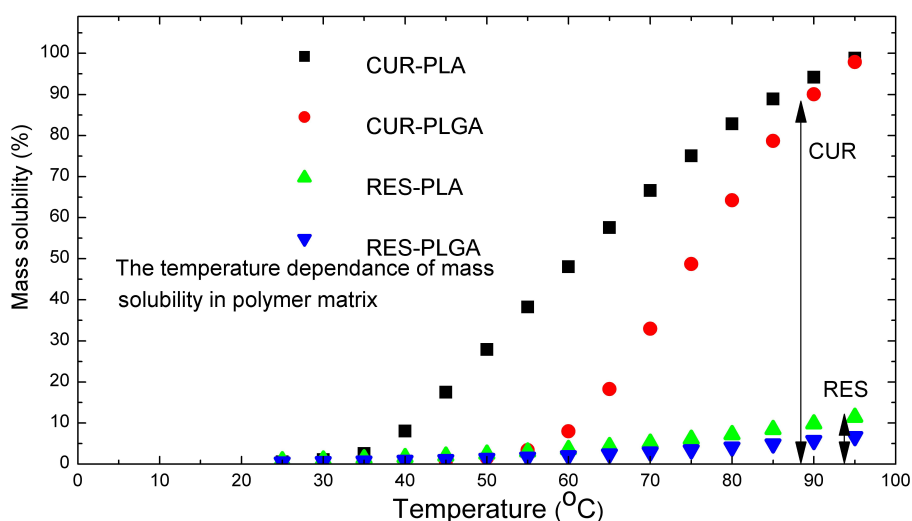
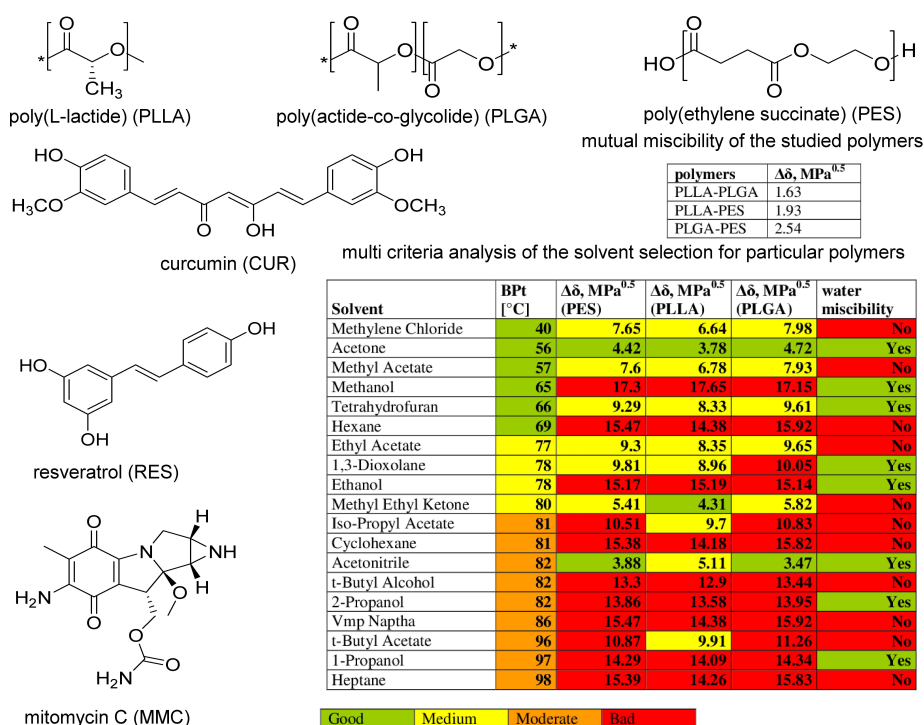


Figure 3. The chemical structures of the studied compounds (CUR, RES, MMC, PLLA, PLGA and PES), mutual compatibility of the polymers, multi criteria selection of the appropriate solvent as well as temperature dependence of mass solubility of CUR and RES.

ones was selected at the median contact angle value. On the other hand, Fujiwara et al. (2019), used an arbitrary contact angle threshold of around 17° to acquire a list of good and bad solvents. This approach is based on an assumption that wettability is equivalent to solubility – a surface with low value of contact angle corresponds to a well soluble substance.

Early attempts to combine wetting angle with HSPs provided numerous equations, satisfied for particular groups of compounds. For example, there were separate formulas for the majority of alcohols, non-alcohols as well as acids, phenols and amines according to Beerbower (1971). On the other hand, Koenhen and Smolders provided a more general relationship, combining δ_D and δ_P values with contact angle for most solvents, with an exception for e.g. acetonitrile, acids and polyols (Koenhen and Smolders, 1975). The division of solvents into alcohols and other groups corresponds to our clusterization studies – the first cluster comprises the majority of compounds with hydroxyl motif, characterized by significant hydrogen bonding – see Section 3. This particular parameter, expressed as δ_H , is underestimated for surface energy according to Koenhen and Smolders (1975), due to the assumption that hydrogen bonds are not broken for interactions involved in liquid-vapor interfacial energy. A similar approach, i.e. determination of relationships for particular groups of common solids and surfaces, e.g. graphite, MoS₂ and WS₂, connected with further generalization is also possible (Jia and Shi, 2011; Yu and Hou, 2019). Such studies enabled to find equations for solids which do not involve the knowledge of the molar volume of liquid.

Surface energy, although not responsible for real adhesion for polymers (Abbott et al., 2020), dependent on polymer chains entangling at the interfacial layer, has a significant impact on choosing of solvents for, especially inorganic, surfaces treatment, e.g. in coating industries or cleaning. This approach is strictly combined with modern calculation methodologies, enabling to group solvents and surfaces into appropriate groups with possible need for separate theoretical and experimental treatment (AlQasas et al., 2023).

5.2. Surface/interface hydrophobization by silicone amphiphiles

Silicones, i.e. macromolecular compounds comprising Si atoms in polymer chains, bonded to each other typically by oxygen, comprising Si–O–Si bridges, or rarely by other chemical motifs (methylene or nitrogen-containing groups), constitute a group of materials with numerous applications, characterized by hydrophobicity, minor reactivity and exceptional stability. Their applications include coatings, anti-adhesives, paints, ink-jet, construction materials, insulations etc. (Hill, 2002). Phthalocyanines comprise a wide group of organic compounds with a planar structure of conjugated aromatic rings and, commonly, a central metal atom. The unique electron structure as well as profound thermal stability (they may be heated even

up to around 400 °C) is a key feature for their applications in energy converting devices, as photosensitizers or additives for enhanced performance at elevated temperatures (Lamch et al., 2021). Although frequently mixed with various organics-based formulations, e.g. lubricants or pastes, they are generally considered as heterogenous when phthalocyanine plays the role of filler or pigment, the incompatibility with the majority of typical organic solvents is well known. The design of materials consisting of phthalocyanines in silicone matrix may be very beneficial, due to thermal stability, protection against unfavorable conditions, especially humidity, as well as chemical resistance. Both phthalocyanines and silicones have not been extensively studied for HSPs, most possibly due to their unique structural features (Si–C and Si–O bonds at various configurations, conjugated aromatic and heteroaromatic rings, planar structures, etc.). On the other hand, the knowledge of mutual compatibility between particular phthalocyanines and silicones is crucial for appropriate design of polymeric host material in order to reduce unnecessary experimental effort.

Therefore, we performed extensive studies of phthalocyanines toward their solubility in organic solvents and compatibility with various silicone structures, utilizing Y–MB approach by HSPiP software. Firstly, HSPs for different phthalocyanines (naphthalocyanine), metallophthalocyanines (zinc (II) phthalocyanine and iron (II) phthalocyanine) and their derivatives (tetra *tert*-butyl phthalocyanine) were calculated for the provided structures in SMILES notation – see Fig. 4. For any of the studied phthalocyanines the predominant type of interactions are London (dispersion) forces, while hydrogen bonding is negligible. For derivatives with central metal atom the share of polar interactions is more significant, when compared with naphthalocyanine without such a motif. On the other hand, such distribution of particular interactions is not common among organic solvents, indicating problems with solubility of numerous phthalocyanines. Therefore, we calculated the values of HSP distance for a set of different solvents, adjacent to all 5 clusters (see Sections 3.5 and 3.6).

The data for 15 best solvents in case of each the studied phthalocyanine are gathered in Table 3. For naphthalocyanine and tetra *tert*-butyl zinc (II) phthalocyanine, i.e. compounds with bulky peripheral groups, the most suitable solvents comprise hydrocarbon-based ones, i.e. cluster “5”, with a few exceptions for, especially, aromatic esters (cluster “2”). Majority of those solvents comprise aromatic or alicyclic rings, providing interactions with peripheral groups in phthalocyanines. On the other hand, zinc (II) and iron (II) phthalocyanines are better soluble in ketones or esters, comprising aromatic or alicyclic moieties, from cluster “2” or, eventually, “3”, although aromatic hydrocarbons (cluster “5”) may also dissolve them. Such findings provide valuable data for further design of silicone-based polymer matrix – generally siloxanes and/or carbosilanes should possess aromatic and/or aliphatic side groups in order to prove superior compatibility with the studied phthalocyanines.

Table 3. Values of HSP distance and attribution to appropriate cluster for the most compatible solvents for each phthalocyanine (for their structures see Fig. 4).

Solvent	Distance $\Delta\delta$, MPa ^{0.5}	Cluster	Solvent	Distance $\Delta\delta$, MPa ^{0.5}	Cluster
NphPc			ZnPc		
Toluene	2.87	5	Benzyl benzoate	7.42	2
p-Cymene	3.29	5	Cyclohexanone	8.3	2
Aromatic Hydrocarbons	3.52	5	Cyrene	8.57	3
Ethyl benzene	3.69	5	Butyl benzoate	8.86	2
Solvesso 150	3.69	5	Propylene carbonate	9.08	3
Solvesso 100	3.81	5	Caprolactone (Epsilon)	9.17	3
Xylene	3.99	5	n-Methyl-2-pyrrolidone	9.55	3
Butyl benzoate	4.63	2	Isophorone	9.61	2
Benzyl benzoate	4.71	2	Dimethyl isosorbide	10.49	2
d-Limonene	4.72	5	1-Nitropropane	10.56	2
Cyclopentyl methyl ether	5.14	5	Toluene	10.74	5
Cyclohexane	5.58	5	p-Cymene	10.86	5
FAME	5.82	5	Anisole	10.94	2
Anisole	5.89	2	Tributyl phosphate	10.97	2
Methyl oleate	6.05	5	Methylene chloride	10.99	2
ZnPc-t-but ₄			FePc		
p-Cymene	3.67	5	Benzyl benzoate	5.74	2
Toluene	4.2	5	Cyclohexanone	6.44	2
Ethyl benzene	4.69	5	Butyl benzoate	6.52	2
Solvesso 150	4.69	5	Isophorone	7.45	2
Solvesso 100	4.71	5	Toluene	7.5	5
Cyclopentyl methyl ether	4.72	5	p-Cymene	7.58	5
Aromatic hydrocarbons	5.06	5	Aromatic hydrocarbons	8.14	5
Xylene	5.08	5	Cyclopentyl methyl ether	8.22	5
Tributyl phosphate	5.19	2	Solvesso 150	8.25	5
Methyl iso-amyl ketone	5.28	2	Ethyl benzene	8.25	5
Cyclohexane	5.41	5	Tributyl phosphate	8.28	2
Di-isobutyl ketone	5.43	5	Solvesso 100	8.4	5
d-Limonene	5.43	5	Anisole	8.55	2
Methyl oleate	5.48	5	Xylene	8.56	5
Butyl benzoate	5.55	2	Dimethyl isosorbide	8.63	2

Compatibility between particular phthalocyanine and polymer matrix may open possibility not only to prepare polymeric materials of appropriate photochemical or electrical properties, but also stable dispersions of phthalocyanine-type derivatives in aqueous systems, when silicone-based amphiphile is used. On the basis of our studies on solvents for phthalocyanines we designed three siloxanes (with Si–O–Si bridges in the main chain) and three carbosilanes (with methylene motifs between

silicone atoms in the main chain) with various numbers of methyl or phenyl side groups per one building block. The distances for particular combinations are provided in Table 4. Moreover, “DIY” menu in HSPiP software enabled to quantitatively calculate weight percent solubility of phthalocyanines in the given polymers – for all combinations there was indefinite (100%) solubility of the payload in polymer matrix.

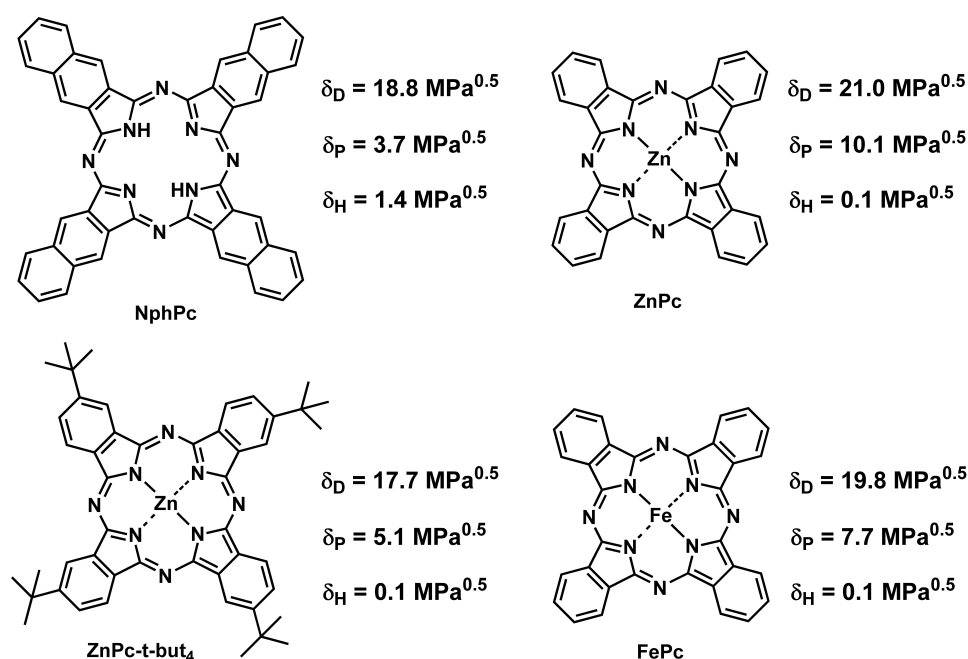


Figure 4. Structures, abbreviations and Hansen solubility parameters for the studied phthalocyanine-type derivatives.

Table 4. HSP distances for particular siloxanes and carbosilanes of the studied phthalocyanines (for their structures see Fig. 4).

Phthalocyanine	siloxanes			carbosilanes		
NphPc	8.49	2.97	2.69	7.95	3.05	2.67
ZnPc	15.60	10.83	9.48	15.13	10.89	9.62
ZnPc-t-but ₄	7.34	4.38	5.41	6.89	4.44	5.32
FePc	12.24	7.59	6.66	11.76	7.66	6.75

Our results clearly show that the introduction of at least one phenyl motif into siloxane or carbosilane significantly enhances solubility of all the studied phthalocyanines in polymer matrix. On the other hand, the difference between appropriate siloxanes and carbosilanes as well as compounds with two phenyl motif was far less significant. Therefore, the design of particular polymers should take into account particular issues: (i) the viscosity of polymers/oligomers and their derivatives, since compounds with exclusively phenyl side groups may be extensively viscous; (ii) susceptibility to undergo hydrolysis of short chained siloxanes, (iii) elasticity of siloxane chains in contrast to carbosilane ones as well as (iv) brittle nature of numerous carbosilanes. Therefore, the compromise structures may constitute siloxanes with one methyl and one phenyl side groups.

HSP studies of phthalocyanines in silicone-based polymeric matrix constitute the first step for the design of numerous functional materials for paint industries, electronic devices,

sensors, catalyst, etc. The use of HSPiP software, combined with appropriate clustering efforts, enabled to reduce unnecessary experimental efforts and decrease the risk of faulty results from traditional solubility probing for phthalocyanines connected with formation of metastable dispersions.

6. CONCLUSIONS

The growing interest of novel materials and processes in chemical nanoengineering, especially in the field of fine and specialty chemicals, constitutes an emerging issue of the design and prediction of crucial physicochemical properties of the given compounds. Therefore, numerous computational and semi-experimental approaches have been studied for such applications, including molecular modeling and machine learning clustering algorithms for data analyses.

Nowadays, one of the most general systems is HSPiP software based on the concept of solubility parameter and group increment approach. The software enables prediction of numerous properties, e.g. solubility parameter (δ) and its components, phase transition temperatures, dependence on mass solubilities on temperature, flash point, partition coefficient and viscosity when the structure of particular compound (even not discovered/synthesized yet!) is known and given as e.g. SMILES notation. Moreover, HSPiP enables obtaining some parameters, especially solubility parameter counterparts of disperse, polar and hydrogen bonding interactions, by various experimental efforts, especially inverse gas chromatography and, most commonly, probing of solubility in various organic solvents.

The use of experimental solubility data for the determination of HSPs is connected with an important issue of particular solvent choice. In order to facilitate this issue, we used clustering algorithms to divide the most popular solvents into a few clusters for statistically more efficient probing toward experimental approach. Moreover, we attributed the obtained clusters of solvents to appropriate features, opening the possibility of explaining experimental results with Hansen solubility parameter theory.

The combination of HSPiP software with proper clustering methodologies enables the support our recent contributions in the fields of novel, multifunctional surfactant synthesis, polymer blends for drug delivery nanosystems, as well as the design of silicone-based host materials for phthalocyanine-type derivatives. Our efforts enabled to facilitate an effective way to find out appropriate solvents for surfactant purification, appropriate polymer blend preparation or phthalocyanine-type derivative dissolving. The potential of HSPiP software provided also possibilities to study other, more subtle, phenomena, e.g. connected with temperature dependent solubility in polymer matrix.

Research case studies, presented in this article, were supported by the National Science Centre of Poland by OPUS Programme (No. 2022/45/B/ST4/01184, part on the multi-charge cationic surfactants) and SONATA Programme (No. 2021/43/D/ST8/01992, HSPiP calculations).

REFERENCES

- Abbott S., Hansen Ch.M., Yamamoto H., 2020. *Hansen solubility parameters in practice*. 5th edition. ISBN 978-0-9551220-2-6.
- Afzal O., Alshammari H.A., Altamimi M.A., Hussain A., Almo-haywi B., Altamimi A.S.A., 2022. Hansen solubility parameters and green nanocarrier based removal of trimethoprim from contaminated aqueous solution. *J. Mol. Liq.*, 361, 119657. DOI: [10.1016/j.molliq.2022.119657](https://doi.org/10.1016/j.molliq.2022.119657).
- AlQasas N., Eskhan A., Johnson D., 2023. Hansen solubility parameters from surface measurements: a comparison of different methods. *Surf. Interfaces*, 36, 102594. DOI: [10.1016/j.surfin.2022.102594](https://doi.org/10.1016/j.surfin.2022.102594).
- Altamimi M.A., Hussain A., Mahdi W.A., Imam S.S., Alshammari M.A., Alshehri S., Khan M.R., 2022. Mechanistic insights into luteolin-loaded elastic liposomes for transdermal delivery: HSPiP predictive parameters and instrument-based evidence. *ACS Omega*, 7, 48202–48214. DOI: [10.1021/acsomega.2c06288](https://doi.org/10.1021/acsomega.2c06288).
- Ash M., Ash I., 2009. *Specialty chemicals source book*. 4th edition, Synapse Information Resources, Incorporated.
- Bapat S., Kilian S.O., Wiggers H., Segets D., 2021. Towards a framework for evaluating and reporting Hansen solubility parameters: applications to particle dispersions. *Nanoscale Adv.*, 3, 4400–4410. DOI: [10.1039/d1na00405k](https://doi.org/10.1039/d1na00405k).
- Barry C.P., Morose G.J., Begin K., Atwater M., Hansen C.J., 2017. The identification and screening of lower toxicity solvents for contact adhesives. *Int. J. Adhes. Adhes.*, 78, 174–181. DOI: [10.1016/j.ijadhadh.2017.06.022](https://doi.org/10.1016/j.ijadhadh.2017.06.022).
- Beerbower A., 1971. Surface free energy: a new relationship to bulk energies. *J. Colloid Interface Sci.*, 35, 126–132. DOI: [10.1016/0021-9797\(71\)90192-5](https://doi.org/10.1016/0021-9797(71)90192-5).
- Bongiardina N.J., Sinha J., Bowman C.N., 2021. Flory–Huggins parameters for thiol-ene networks using Hansen solubility parameters. *Macromolecules*, 54, 11439–11448. DOI: [10.1021/acs.macromol.1c01957](https://doi.org/10.1021/acs.macromol.1c01957).
- Chen Y., Wang Q., Zhang Z., Tang J., 2012. Determination of the solubility parameter of ionic liquid 1-hexyl-3-methylimidazolium hexafluorophosphate by inverse gas chromatography. *Ind. Eng. Chem. Res.*, 51, 15293–15298. DOI: [10.1021/ie301924y](https://doi.org/10.1021/ie301924y).
- Chollet F., 2021. *Deep learning with Python*. 2nd edition, Manning Publications Co. LLC, New York.
- Ciriminna R., Della Pina C., Luque R., Pagliaro M., 2024. Reshoring fine chemical and pharmaceutical productions. *Org. Process Res. Dev.*, 28, 3026–3034. DOI: [10.1021/acs.oprd.4c00219](https://doi.org/10.1021/acs.oprd.4c00219).
- Díaz de los Ríos M., Hernández Ramos E., González Canavaciolo V., González Murillo R., Pérez Carrión K., Zumalacarregui de Cárdenas L., 2022. Obtaining a fraction of dugarcane wax rich in policosanol by using ethanol as solvent: results interpretation through Hansen's solubility theory. *ACS Omega*, 7, 27324–27333. DOI: [10.1021/acsomega.2c02314](https://doi.org/10.1021/acsomega.2c02314).
- Fujiwara N., Nishida T., Yamamoto H., 2019. Adaptation of Hansen solubility parameter in evaluating transparency of composite materials. *Heliyon*, 5, e02833. DOI: [10.1016/j.heliyon.2019.e02833](https://doi.org/10.1016/j.heliyon.2019.e02833).
- Gerzona G., Shenga Y., Kirkitadze M., 2022. Process analytical technologies – advances in bioprocess integration and future perspectives. *J. Pharm. Biomed. Anal.*, 207, 114379. DOI: [10.1016/j.jpba.2021.114379](https://doi.org/10.1016/j.jpba.2021.114379).
- Hansen C.M., 2000. *Hansen solubility parameters: A user's handbook*. CRC Press,
- Hill R.M., 2002. Silicone surfactants – new developments. *Curr. Opin. Colloid Interface Sci.*, 7, 255–261. DOI: [10.1016/S1359-0294\(02\)00068-7](https://doi.org/10.1016/S1359-0294(02)00068-7).
- Hussain A., Altamimi M.A., Ramzan M., Mirza M.A., Khuroo T., 2023a. GastroPlus- and HSPiP-oriented predictive parameters as the basis of valproic acid-loaded mucoadhesive cationic nanoemulsion gel for improved nose-to-brain delivery to control convulsion in humans. *Gels*, 9, 603. DOI: [10.3390/gels9080603](https://doi.org/10.3390/gels9080603).

- Hussain A., Altamimi M.A., Sarim Imam S., Imam F., 2023b. Green nanoemulsion-based treatment to remove sulfamethoxazole from a contaminated water solution. *J. Mol. Liq.*, 384, 122183. DOI: [10.1016/j.molliq.2023.122183](https://doi.org/10.1016/j.molliq.2023.122183).
- Hussain A., Ramzan M., Altamimi M.A., Khuroo T., 2023c. HSPiP and QbD program-based analytical method development and validation to quantify ketoconazole in dermatokinetic study. *AAPS PharmSciTech*, 24, 231. DOI: [10.1208/s12249-023-02675-9](https://doi.org/10.1208/s12249-023-02675-9).
- Hussain A., Sarim Imam S., Altamimi M.A., Shahid M., Alnemer O.A., 2023d. Optimized green nanoemulsions to remove pharmaceutical enoxacin from contaminated bulk aqueous solution. *ACS Omega*, 8, 11100–11117. DOI: [10.1021/acsomega.2c07942](https://doi.org/10.1021/acsomega.2c07942).
- Jia L., Shi B., 2011. A new equation between surface tensions and solubility parameters without molar volume parameters simultaneously fitting polymers and solvents. *J. Macromol. Sci. Part B Phys.*, 50, 1042–1046. DOI: [10.1080/00222348.2010.497439](https://doi.org/10.1080/00222348.2010.497439).
- Jiang X., Wang W., Li M., 2014. Selecting water-alcohol mixed solvent for synthesis of polydopamine nano-spheres using solubility parameter. *Sci. Rep.*, 4, 6070. DOI: [10.1038/srep06070](https://doi.org/10.1038/srep06070).
- Jiang X., Yuan X., Guo X., Zeng, F., Liu G., 2022. Determination of three-dimensional solubility parameters of HNBR/EPDM blends and the transport behaviors in ester solvents. *J. Appl. Polym. Sci.*, 139, e52881. DOI: [10.1002/app.52881](https://doi.org/10.1002/app.52881).
- Kobayashi Y., Tokishita S., Yamamoto H., 2020. Determination of Hansen solubility parameters of ionic liquids by using Walden plots. *Ind. Eng. Chem. Res.*, 59, 14217–14223. DOI: [10.1021/acs.iecr.0c01947](https://doi.org/10.1021/acs.iecr.0c01947).
- Koehn D.M., Smolders C.A., 1975. The determination of solubility parameters of solvents and polymers by means of correlations with other physical quantities. *J. Appl. Polym. Sci.*, 19, 1163–1179. DOI: [10.1002/app.1975.070190423](https://doi.org/10.1002/app.1975.070190423).
- Kohonen T., 1982. Self-organized formation of topologically correct feature maps. *Biol. Cybern.*, 43, 59–69. DOI: [10.1007/BF00337288](https://doi.org/10.1007/BF00337288).
- Kohonen T., 2013. Essentials of the self-organizing map. *Neural Networks*, 37, 52–65. DOI: [10.1016/j.neunet.2012.09.018](https://doi.org/10.1016/j.neunet.2012.09.018).
- Laboukhi-Khorsi S., Daoud K., Chemat S., 2017. Efficient solvent selection approach for high solubility of active phytochemicals: application for the extraction of an antimalarial compound from medicinal plants. *ACS Sustainable Chem. Eng.*, 5, 4332–4339. DOI: [10.1021/acssuschemeng.7b00384](https://doi.org/10.1021/acssuschemeng.7b00384).
- Lamch Ł., Gancarz R., Tsirigotis-Maniecka M., Moszyńska I.M., Ciejka J., Wilk K.A., 2021. Studying the „rigid-flexible” properties of polymeric micelles core-forming segments by a hydrophobic phthalocyanine probe using NMR and UV spectroscopies. *Langmuir*, 37, 4316–4330. DOI: [10.1021/acs.langmuir.1c00328](https://doi.org/10.1021/acs.langmuir.1c00328).
- Lamch Ł., Leszczyńska I., Długowska D., Szczęśna-Górnaiak W., Batys P., Jarek E., Wilk K.A., Warszński P., 2025. Synthesis of new cationic dicephalic surfactants and their nonequivalent adsorption at the air/solution interface. *Langmuir*, 41, 8125–8137. DOI: [10.1021/acs.langmuir.4c04803](https://doi.org/10.1021/acs.langmuir.4c04803).
- Lamch Ł., Pucek A., Kulbacka J., Chudy M., Jastrzębska E., Tokarska K., Bułka M., Brzózka Z., Wilk K.A., 2018. Recent progress in the engineering of multifunctional colloidal nanoparticles for enhanced photodynamic therapy and bioimaging. *Adv. Colloid Interface Sci.*, 261, 62–81. DOI: [10.1016/j.cis.2018.09.002](https://doi.org/10.1016/j.cis.2018.09.002).
- Lamch Ł., Szczęśna W., Balicki S.J., Bartman M., Szyk-Warszyńska L., Warszński P., Wilk K.A., 2023. Multiheaded cationic surfactants with dedicated functionalities: design, synthetic strategies, self-assembly and performance. *Molecules*, 28, 5806. DOI: [10.3390/molecules28155806](https://doi.org/10.3390/molecules28155806).
- Lamch Ł., Szklarz P., 2024. Effect of temperature and composition on the loading of curcumin into PLGA/PLLA core-shell nanoparticles stabilized by hydrophobically functionalized polyelectrolytes. *Ind. Eng. Chem. Res.*, 63, 10279–10290. DOI: [10.1021/acs.iecr.4c01417](https://doi.org/10.1021/acs.iecr.4c01417).
- Lamch Ł., Szukiewicz R., 2024. Entrapment of amphipathic drugs in core-shell polymeric nanoparticles under batch conditions – the role of control and solubility parameters. *Langmuir*, 40, 21186–21198. DOI: [10.1021/acs.langmuir.4c02721](https://doi.org/10.1021/acs.langmuir.4c02721).
- Lan Y., Corradini M.G., Liu X., May T.E., Borondics F., Weiss R.G., Rogers M.A., 2014. Comparing and correlating solubility parameters governing the self-assembly of molecular gels using 1,3:2,4-dibenzylidene sorbitol as the gelator. *Langmuir*, 30, 14128–14142. DOI: [10.1021/la5008389](https://doi.org/10.1021/la5008389).
- Lazghab M., Saleh K., Pezron I., Guigon P., Komunjer L., 2005. Wettability assessment of finely divided solids. *Powder Technol.*, 157, 79–91. DOI: [10.1016/j.powtec.2005.05.014](https://doi.org/10.1016/j.powtec.2005.05.014).
- Ledakowicz S., Antecka A., Gluszczyński P., Klepacz-Smolka A., Pietrzyk D., Szeląg R., Slezak R., Daroch M., 2024. From 3G biofuels to high-value-added bioproducts. *Chem. Proc. Eng. New Front.*, 45, e59. DOI: [10.24425/cpe.2024.148553](https://doi.org/10.24425/cpe.2024.148553).
- Li C., Li Z., Liu X., Xu J., Zhang C., 2024. Machine learning approach to predict Hansen solubility parameters of cocrystal cofomers via integrating group contribution and COSMO-RS. *J. Mol. Liq.*, 408, 125319. DOI: [10.1016/j.molliq.2024.125319](https://doi.org/10.1016/j.molliq.2024.125319).
- Malpani V., Ganeshpure P.A., Munshi P., 2011. Determination of solubility parameters for the p-xylene oxidation products. *Ind. Eng. Chem. Res.*, 50, 2467–2472. DOI: [10.1021/ie101623c](https://doi.org/10.1021/ie101623c).
- Milescu R.A., Segatto M.L., Stahl A., McElroy C.R., Farmer T.J., Clark J.H., Zuin V.G., 2020. Sustainable single-stage solid-liquid extraction of hesperidin and rutin from agro-products using cyrene. *ACS Sustainable Chem. Eng.*, 8, 18245–18257. DOI: [10.1021/acssuschemeng.0c06751](https://doi.org/10.1021/acssuschemeng.0c06751).
- Mostafa E.A., Azim M.A., ElZaher A.A., ElKady E.F., Fouad M.A., Ghazy F.H., Radi E.A., El Makarim Saleh M.A., El Kerdawy A.M., 2024. Correlating physico-chemical properties of analytes with Hansen solubility parameters of solvents using machine learning algorithm for predicting suitable extraction solvent. *Sci. Rep.*, 14, 18741. DOI: [10.1038/s41598-024-68981-9](https://doi.org/10.1038/s41598-024-68981-9).
- Novo L.P., Curvelo A.A.S., 2019. Hansen solubility parameters: a tool for solvent selection for organosolv delignification. *Ind. Eng. Chem. Res.*, 58, 14520–14527. DOI: [10.1021/acs.iecr.9b00875](https://doi.org/10.1021/acs.iecr.9b00875).

- Patel A.A., 2019. *Hands-on unsupervised learning using Python. How to build applied machine learning solutions from unlabeled data*. O'Reilly Media, Sebastopol, CA.
- Patil T., Siddique M.U.M., Shelke M., Ramzan M., Patil M., Shahid M., 2024. Development and validation of HSPiP- and optimization-assisted method to analyze tolterodine tartrate in pharmacokinetic study. *Processes*, 12, 2164. DOI: [10.3390/pr12102164](https://doi.org/10.3390/pr12102164).
- Petchey T.H.M., Comerford J.W., Farmer T.J., Macquarrie D.J., Sherwood J., Clark J.H., 2018. Optimization of amidation reactions using predictive tools for the replacement of regulated solvents with safer biobased alternatives. *ACS Sustainable Chem. Eng.*, 6, 1550–1554. DOI: [10.1021/acssuschemeng.7b04257](https://doi.org/10.1021/acssuschemeng.7b04257).
- Pollak P., 2011. *Fine Chemicals. The industry and the business*. Wiley, Hoboken, 26–48.
- Qin J., Wang X., Jiang Q., Cao M., 2019. Optimizing dispersion, exfoliation, synthesis, and device fabrication of inorganic nanomaterials using Hansen solubility parameters. *ChemPhysChem*, 20, 1069–1097. DOI: [10.1002/cphc.201900110](https://doi.org/10.1002/cphc.201900110).
- Sels H., De Smet H., Geuens J., 2020. *SUSSOL* — using artificial intelligence for greener solvent selection and substitution. *Molecules*, 25, 3037. DOI: [10.3390/molecules25133037](https://doi.org/10.3390/molecules25133037).
- Shakeel F., Haq N., Alsarra I., Alshehri S., 2021a. Solubility data, solubility parameters and thermodynamic behavior of an antiviral drug emtricitabine in different pure solvents: molecular understanding of solubility and dissolution. *Molecules*, 26, 746. DOI: [10.3390/molecules26030746](https://doi.org/10.3390/molecules26030746).
- Shakeel F., Haq N., Alsarra I.A., 2021b. Equilibrium solubility determination, Hansen solubility parameters and solution thermodynamics of cabozantinib malate in different monosolvents of pharmaceutical importance. *J. Mol. Liq.*, 324, 115146. DOI: [10.1016/j.molliq.2020.115146](https://doi.org/10.1016/j.molliq.2020.115146).
- Soyemi A., Szilvási T., 2023. Calculated physicochemical properties of glycerol-derived solvents to drive plastic waste recycling. *Ind. Eng. Chem. Res.*, 62, 6322–6337. DOI: [10.1021/acs.iecr.2c04567](https://doi.org/10.1021/acs.iecr.2c04567).
- Szarpak D., Lamch Ł., Szczęśna-Górniak W., Warszyński P., Wilk K.A., 2024. Determination of Hansen solubility parameters of novel cationic dicephalic surfactants. *ECIS 2024*, Copenhagen, Denmark, 1–6 July 2024.
- Szczęśna W., Ciejka J., Szyk-Warszyńska L., Jarek E., Wilk K.A., Warszyński P., 2022. Customizing polyelectrolytes through hydrophobic grafting. *Adv. Colloid Interface Sci.*, 306, 102721. DOI: [10.1016/j.cis.2022.102721](https://doi.org/10.1016/j.cis.2022.102721).
- Tripathi A., Parsons G.N., Khan S.A., Rojas O.J., 2018. Synthesis of organic aerogels with tailorable morphology and strength by controlled solvent swelling following Hansen Solubility. *Sci. Rep.*, 8, 2106. DOI: [10.1038/s41598-018-19720-4](https://doi.org/10.1038/s41598-018-19720-4).
- Tsutsumi S., Kato Y., Namba K., Yamamoto H., 2019. Functional composite material design using Hansen solubility parameters. *Res. Mater.*, 4, 100046. DOI: [10.1016/j.rinma.2019.100046](https://doi.org/10.1016/j.rinma.2019.100046).
- van Krevelen D.W., 2009. *Properties of polymers*. Elsevier B.V.
- Venkatesan K., Haider N., Yusuf M., Hussain A., Afzal O., Yamin S., Altamimi A.S.A., 2022. Water/transcutol/lecithin/M-812 green cationic nanoemulsion to treat oxytetracycline contaminated aqueous bulk solution. *J. Mol. Liq.*, 357, 119154. DOI: [10.1016/j.molliq.2022.119154](https://doi.org/10.1016/j.molliq.2022.119154).
- Wang Q., Chen Y., Zhang Z., Tang J., 2013. Determination of surface characteristics of ionic liquid [1-hexyl-3-methylimidazolium hexafluorophosphate] by inverse gas chromatography. *J. Chem. Eng. Data*, 58, 2142–2146. DOI: [10.1021/je3012327](https://doi.org/10.1021/je3012327).
- Warszyński P., Szyk-Warszyńska L., Wilk K.A., Lamch Ł., 2022. Adsorption of cationic multicharged surfactants at liquid–gas interface. *Curr. Opin. Colloid Interface Sci.*, 59, 101577. DOI: [10.1016/j.cocis.2022.101577](https://doi.org/10.1016/j.cocis.2022.101577).
- Weźgowiec J., Łapińska Z., Lamch Ł., Szewczyk A., Sączko J., Kulbacka J., Więckiewicz M., Wilk K.A., 2025. Cytotoxic activity of curcumin and resveratrol loaded core-shell systems in resistant and sensitive human ovarian cancer cells. *Int. J. Mol. Sci.*, 26, 41. DOI: [10.3390/ijms26010041](https://doi.org/10.3390/ijms26010041).
- Wieneke J.U., Kommoß B., Gaer O., Prykhodko I., Ulbricht M., 2012. Systematic investigation of dispersions of unmodified inorganic nanoparticles in organic solvents with focus on the Hansen solubility parameters. *Ind. Eng. Chem. Res.*, 51, 327–334. DOI: [10.1021/ie201973u](https://doi.org/10.1021/ie201973u).
- Wojeicichowski J.P., Ferreira A.M., Okura T., Pinheiro Rolemberg M., Mafra M.R., Coutinho J.A.P., 2022. Using COSMO-RS to predict Hansen solubility parameters. *Ind. Eng. Chem. Res.*, 61, 15631–15638. DOI: [10.1021/acs.iecr.2c01592](https://doi.org/10.1021/acs.iecr.2c01592).
- Yin H., Takada K., Kumar A., Hirayama T., Kaneko T., 2021. Synthesis and solvent-controlled self-assembly of diketopiperazine-based polyamides from aspartame. *RSC Adv.*, 11, 5938–5946. DOI: [10.1039/d0ra10086b](https://doi.org/10.1039/d0ra10086b).
- Yu S., Sharma R., Morose G., Nagarajan R., 2021. Identifying sustainable alternatives to dimethyl formamide for coating applications using Hansen solubility parameters. *J. Cleaner Prod.*, 322, 129011. DOI: [10.1016/j.jclepro.2021.129011](https://doi.org/10.1016/j.jclepro.2021.129011).
- Yu W., Hou W., 2019. Correlations of surface free energy and solubility parameters for solid substances. *J. Colloid Interface Sci.*, 544, 8–13. DOI: [10.1016/j.jcis.2019.02.074](https://doi.org/10.1016/j.jcis.2019.02.074).
- Zhang W., Ma X., Yang C., Ni C., Pang Z., Li X., Yang Z., 2024. Hansen solubility parameters sphere calculations and thermodynamic model fitting of two novel copper complexes supported by bis(imino) pyridine ligands. *J. Mol. Liq.*, 395, 123593. DOI: [10.1016/j.molliq.2023.123593](https://doi.org/10.1016/j.molliq.2023.123593).
- Zhou W.-J., Metivier P., 2023. Science – an important lever to tackle sustainability in the specialty chemical industry. *Natl. Sci. Rev.*, 10, nwad193. DOI: [10.1093/nsr/nwad193](https://doi.org/10.1093/nsr/nwad193).
- Zhu Q.-N., Wang Q., Hu Y.-B., Abliz X., 2019. Practical determination of the solubility parameters of 1-alkyl-3-methylimidazolium bromide ([C_nC₁im]Br, n = 5, 6, 7, 8) ionic liquids by inverse gas chromatography and the Hansen solubility parameter. *Molecules*, 24, 1346. DOI: [10.3390/molecules24071346](https://doi.org/10.3390/molecules24071346).

Chemical Engineering Horizons and Perspectives.

Article series endorsed by the Scientific Committee on Chemical and Process Engineering of the Polish Academy of Sciences, term 2024–2027